



Optimization of P compounds recovery from aerobic sludge by chemical modeling and response surface methodology combination

Saba Daneshgar^{a,b}, Peter A. Vanrolleghem^b, Céline Vaneckhaute^{b,c},
Armando Buttafava^d, Andrea G. Capodaglio^{a,*}

^a Department of Civil Engineering and Architecture, University of Pavia, Pavia, Italy

^b modelEAU, Département de génie civil et de génie des eaux, Université Laval, Québec City, Québec, Canada

^c BioEngine, Research Team on Green Process Engineering and Biorefineries, Chemical Engineering Department, Université Laval, Québec City, Québec, Canada

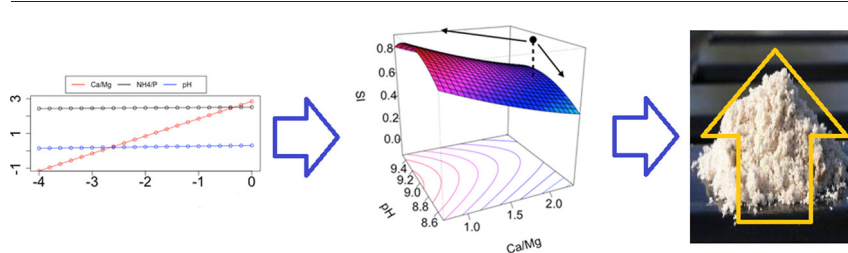
^d UNE.CO srl, Academic Spinoff, Pavia, Italy



HIGHLIGHTS

- P recovery should be preferred to removal in wastewater systems, for sustainability.
- Various valuable P forms may be precipitated from a WWTP, depending on conditions.
- Experimental and statistical analyses were applied to assess recovery optimization.
- Optimized values of process variables will lead to more efficient P recovery.

GRAPHICAL ABSTRACT



ARTICLE INFO

Article history:

Received 31 December 2018

Received in revised form 4 March 2019

Accepted 4 March 2019

Available online 05 March 2019

Editor: Frederic Coulon

Keywords:

Phosphorous removal
Phosphorous recovery
Wastewater
Struvite
Phosphates
Modeling
Optimization

ABSTRACT

Phosphorus recovery has drawn much attention during recent years, due to estimated limited available quantities, and to the harmful environmental impact that it may have when freely released into aquatic environments. Struvite precipitation from wastewater or biological sludge is among the preferred approaches applied for phosphorus recovery, as it results in the availability of valuable fertilizer materials. This process is mostly affected by pH and presence of competitive ions in solution. Modeling and optimization of the precipitation process may help understanding the optimal conditions under which the most efficient recovery could be achieved. In this study, a combination of chemical equilibrium modeling and response surface methodology (RSM) was applied to this aim to aerobic sludge from a plant in Italy. The results identify optimum chemical parameters values for best phosphorus precipitation recovery and removal efficiencies, respectively. Identification of optimal conditions for process control is of great importance for implementing pilot scale struvite precipitation and achieve efficient phosphorus recovery.

© 2019 Elsevier B.V. All rights reserved.

1. Introduction

Phosphorus is perhaps the most essential nutrient for all living organisms on Earth, widely found in nature mostly in phosphate form,

due to the high reactivity of its elemental form. In spite of its biological importance (i.e. as element allowing crop and plant growth), it can also generate serious environmental problems when freely released into water bodies (Bendoricchio et al., 1993; Capodaglio et al., 2003). Phosphorus also generates important sustainability concerns as it is a finite and nonrenewable resource (Cordell et al., 2009; Daneshgar et al., 2018a), making its recovery a desirable goal, whenever possible.

* Corresponding author.

E-mail address: andrea.capodaglio@unipv.it (A.G. Capodaglio).

Nowadays, combining its removal and recovery from wastewater streams seems an appropriate and often feasible strategy.

Phosphorus recovery technologies have been studied for many years, and different approaches for achieving that have been proposed (Desmidt et al., 2015; Peng et al., 2018). The most common method is the (non-metal) precipitation process (Daneshgar et al., 2018b), the product of which could be in the form of calcium phosphate compounds or most notably magnesium ammonium phosphate hexahydrate ($MgNH_4PO_4 \cdot 6H_2O$), also called “Struvite”. This is an invaluable mineral that, due to its low solubility, slow release, low metal and high nutrient (P and also N) contents could be considered a suitable fertilizer. Different parameters impact the efficiency of struvite precipitation, such as pH and concentration of constituent ions. Many studies have investigated the process of struvite precipitation and its modeling and optimization in order to achieve high levels of phosphorus recovery. Wang et al. (2005) studied the theoretical optimum values for pH that may lead to higher process efficiency (finding them within the range 8.5–9.5). Le Corre et al. (2007) investigated the kinetics of struvite crystallization reactions, showing that they are affected by the initial concentration of magnesium in the solution. Bhuiyan et al. (2007) studied with great detail struvite thermodynamics, and in particular its solubility at different temperatures and pH. There have been studies on the use of fluidized-bed reactors for struvite crystallization, and investigations on related reaction parameters (Bhuiyan et al., 2008). Morse et al. (1998) conducted a comprehensive review on struvite formation and its different recovery methods.

In addition, studies have been conducted on modeling and optimization of the struvite precipitation process using chemical speciation modeling tools, such as PHREEQC (US Geological Survey, 2013) and MINTQA2 (US EPA, 1991). Such models are capable of calculating ion speciation, saturation index, equilibrium conditions, ionic strength, etc. based on the initial conditions of a solution or mixture of solutions. Possible solid phases and related occurring reactions in the system may also be simulated. Lee et al. (2013) developed an equilibrium model for struvite formation and precipitation with calcium co-precipitation. Türker and Çelen (2007) used chemical equilibrium to predict ammonia removal in the form of struvite from anaerobic digester effluent. Harada et al. (2006) predicted struvite formation from urine using a new equilibrium model and considering co-precipitation of calcium phosphate compounds and carbonates.

Struvite precipitation can also be modeled and optimized using statistical approaches. Statistical modeling is a powerful class of tools to investigate possible relationships between variables affecting a process and those describing its efficiency. Establishing such relationships helps process engineers to implement future process designs in more efficient and possibly cost-effective ways. Statistical modeling approaches are basically a way to detect significant effects of process inputs onto process outputs. Further steps in such approaches could lead to finding an optimum range of the operating parameters, fitting a model in the form of $y = f(x)$ where y is the process output or response variable and x is a set of process parameters or predictor variables. Response surface methodology (RSM) is a well-known statistical approach to this aim object of a few interesting works were conducted during the past decade (Capdevielle et al., 2013; de Luna et al., 2015; Shalaby, 2015; Ye et al., 2016; Munir et al., 2017). RSM was introduced in 1951 by George E.P. Box and K.B. Wilson (Box and Wilson, 1951), based on using a set of designed experiments to optimize a response variable. An advantage of using RSM is that it allows to understand the impact of changes in the degrees of freedom on the optimum result, and can help investigate the direction of changing predictor variables needed to move towards, in order to maximize or minimize response variables. Shalaby (2015) investigated optimization of phosphorus removal from industrial and synthetic wastewater streams using pH, temperature, reaction time and ion molar ratios as predictor variables. de Luna et al. (2015) used pH, initial phosphorus concentration and magnesium-to-phosphorus molar ratio in order to

optimize a multi-response system, considering total and dissolved phosphate, magnesium and ammonium removal percentages as response variables. Capdevielle et al. (2013) considered also the reaction stirring rate, and the presence of calcium among predictor variables, and studied the optimization of phosphorus removal, particle size and struvite to calcium phosphate ratio.

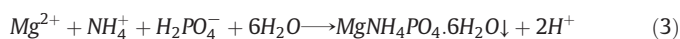
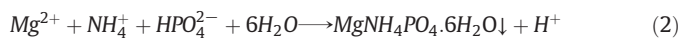
This study investigates simulation and subsequent optimization of struvite precipitation from a municipal wastewater stream by combining chemical equilibrium modeling with RSM's statistical approach. Chemical equilibrium models were used to complement previous experimental work by calculating ion speciation and saturation index (SI) values for struvite. Results were then further used as input data for an RSM approach, to optimize both phosphorus removal percentage and struvite's SI, helping determine optimum response values for new sets of conditions without previously calculating them through chemical equilibrium calculations. Although many studies are available on struvite chemical equilibrium modeling, few valuable studies on the application of RSM for process optimization exist, and there is a general lack of those in which advantage is taken by combining both methods for an overall better understanding of struvite precipitation, and its optimization in terms of simultaneous maximum phosphorus removal and struvite crystallization.

2. Struvite chemistry, kinetics and thermodynamics

Struvite precipitation occurs according to the following reaction:



However, phosphate in solution may also be present in HPO_4^{2-} and $H_2PO_4^-$ forms, contributing to struvite formation according to Eqs. (2) and (3):



In reality, Eq. (2) is dominant compared to the others for the pH range in which struvite formation is favorable (7–11) (Doyle and Parsons, 2002). Therefore, it is important to take all reactions, and particularly the reaction of HPO_4^{2-} into account in the study of struvite precipitation.

Important factors affecting this process are pH, concentrations of constituent ions and presence of competitive ions, most notably Ca^{2+} (Hao et al., 2008). Struvite precipitation might take place spontaneously at different locations of a wastewater treatment facility and consequently could lead to specific unwanted problems such as pumps, pipes and valves clogging (Borgerding, 1972). However, controlled occurrence of the reaction could be a very effective method for recovering phosphorus.

The mechanism of struvite crystallization can be categorized in three steps: nucleation, crystal growth and aggregation (Galbraith et al., 2014; Le Corre et al., 2007). Nucleation is the formation of small crystals of struvite followed by crystal growth, which is the development of the small sized crystal into larger ones. Aggregation occurs when several crystals come together and form some sort of clusters. Such mechanisms are affected by many factors such as pH, thermodynamics of the system, kinetics of the reaction, initial ionic concentration, temperature, etc. (Le Corre, 2006). Studies on struvite precipitation kinetics suggest that these three reaction steps could all be empirically formulated as a function of the struvite supersaturation ratio (Galbraith and Schneider, 2014; Vaneekhaute et al., 2018). The latter is basically the ion activity product (IAP) of constituent ions in solution over its equilibrium solubility product (K_{sp}). A solution is supersaturated when ionic concentrations are above their equilibrium levels, and consequently precipitation may occur to return the system into equilibrium

conditions. Similarly, when ion concentrations are below equilibrium level, the system is called undersaturated, and precipitation will not occur. Eq. (4) formulates the “Saturation Index” concept, which is the logarithm of the supersaturation ratio (Parkhurst and Appelo, 2013):

$$IAP = \{Mg^{2+}\} \{NH_4^+\} \{PO_4^{3-}\} \quad (4)$$

$$SI = \log\left(\frac{IAP}{K_{sp}}\right) \quad (5)$$

Basically, when $SI > 0$ the system is supersaturated and when $SI < 0$, it will be in undersaturated condition. $SI = 0$ means that the system is at equilibrium.

Investigations on thermodynamics and kinetics of struvite precipitation may be carried out experimentally (Bhuiyan et al., 2007; Galbraith et al., 2014). However, chemical equilibrium modeling tools (e.g. the previously mentioned PHREEQC and MINTEQA2) may also be used to that end, with the advantage of faster achievement of results, while predicting accurate equilibrium conditions and ion speciation based on initial solution conditions.

3. Materials and methods

3.1. Sludge characteristics

Sludge samples from a municipal wastewater treatment facility in Milan (Italy), one of the largest in northern Italy, were collected for this study. The facility, serving over 1 million P.E. and producing approximately 50,000 t/yr of biological sludge, containing an estimated 1400 t/yr of phosphorus, has a considerable potential for P recovery due to its specific setup and operational conditions (Daneshgar et al., 2018b). Mixed liquor samples were taken from the inlet zone of the main oxidation tank, where the highest concentration of phosphorus is observed due to its release in the preceding anaerobic stage, and therefore where the highest potential of struvite precipitation may occur. Table 1 shows the main (average) characteristics of collected samples.

3.2. Analytical methods

Phosphorus concentrations were measured according to colorimetric method EPA 365.3 (US EPA, 1978) using UV-Vis spectroscopy (HP 8452A Diode Array Spectrophotometer). The samples were first filtered using 2.5 μ m filters and P determinations were made on the solution phase. The precipitates obtained in each experiment were washed with deionized water and dried at room temperature. Analysis of the precipitates was conducted using Fourier Transform Infrared (FTIR) spectroscopy (Perkin Elmer 1600 series), Thermal Gravimetric Analysis (TGA) (Mettler Toledo TGA 1 STARe System), Mass Spectroscopy (MS), Inductively Coupled Plasma Atomic Emission Spectroscopy (ICP-AES) and Elemental Analysis to identify different solid phases in the final precipitates.

Table 1
Mixed liquor characteristics.

Ions	Concentrations* (mg/l)
Ca ²⁺	101
Mg ²⁺	26.4
P*	40.3
NH ₄ ⁺	32.6

* Solution-phase.

3.3. Experimental setup

Initial experiments were performed in laboratory on the filtered solution using 200 ml beakers. A solution of NaOH was used to adjust pH, while MgCl₂ and NH₄Cl were used as sources of magnesium and ammonium, respectively, when adjusting ionic ratios in the tested solution. Moderate aeration was used to provide some liquor mixing in all experiments. Final precipitates were collected after 20 h in order to allow the process to reach equilibrium. The solutions were then filtered with 0.45 μ m filters to separate the precipitate, dried at room temperature prior to FTIR analysis. P measurements were conducted on the final filtrate.

3.4. Chemical equilibrium modeling using PHREEQC

The PHREEQC model, a widely used geochemical software tool designed by the US Geological Survey (USGS), is capable of performing a wide variety of aqueous calculations such as ion speciation batch reactions and calculating saturation index (SI) values based on the solution characteristics (ion concentrations, pH, etc.) as input. In this study, PHREEQC version 3.0 was used to model chemical equilibria.

3.4.1. PHREEQC database modification

PHREEQC includes different databases describing different species with their corresponding reactions and solid phases precipitated in the final product. The default PHREEQC.DAT database, was selected in this study; however, as it is not optimized for the specific case of struvite precipitation, it needed to be modified. The K_{sp} of struvite used in PHREEQC modeling was taken from Taylor et al. (1963) ($K_{sp} = 13.26$). As there are several solid phases that could theoretically precipitate in such a system, however, with precipitation highly dependent on process operating conditions, some missing solid phases and their equilibrium equations were added to the model database, and some unnecessary phases deemed highly unlikely to precipitate were removed from it (Daneshgar et al., 2018c). Table 2 shows the list of solid phases that were included in the database of PHREEQC for this study.

3.4.2. Model operation

Concentrations of all available ions were fed to the PHREEQC model as input for calculations. pH levels, and the amount of NaOH added to the system to adjust its value were also included. The output of the model consists of ion speciation and saturation index (SI) values for each of the solid phases defined in the database. Ion speciation data were separately used to calculate phosphorus removal percentage for each of the experiments.

3.5. Statistical modeling

3.5.1. Response surface methodology (RSM)

Statistical testing was conducted according to the Box-Behnken Design (BBD). BBD is a specific type of experimental design introduced in 1960 (Box and Behnken, 1960), used for Response Surface Methodology (RSM) analysis applications. It uses factors with at least three levels (maximum, minimum and center point) for each experimental variable and fits a second order polynomial model to the data. Fig. 1 shows the schematics of the Box-Behnken Design for 3 factors, and the points at which the experiments need be performed. BBD methodology needs 15 experiments for obtaining three predictor variables, as was the case for our study. The levels of pH, calcium to magnesium molar ratio (Ca²⁺/Mg²⁺) and ammonium to phosphorus molar ratio (NH₄⁺/P) have been chosen as the three predictor variables to optimize struvite saturation index (SI) and phosphorus removal percentage as response variables. Table 3 shows the 15 runs of numerical experiments with their associated levels for each factor, chosen based on prior precipitation experiments. The initial values of the Ca/Mg and NH₄/P molar ratios were 2.33 and 1.5 respectively: the former is already quite high, and will make calcium very competitive for phosphate precipitation in the

Table 2List of solid phases included in the database of PHREEQC software with their corresponding K_{sp} values.

Solid phase	Reaction	pK_{sp} at 25 °C	Reference
Struvite	$Mg^{2+} + NH_4^+ + PO_4^{3-} + 6H_2O \leftrightarrow MgNH_4PO_4 \cdot 6H_2O$	13.26	(Taylor et al., 1963)
Monetite (DCP)	$Ca^{2+} + HPO_4^{2-} \leftrightarrow CaHPO_4$	6.81	(Johnsson and Nancollas, 1992)
Amorphous calcium phosphate (ACP)	$3Ca^{2+} + 2PO_4^{3-} + xH_2O \leftrightarrow Ca_3(PO_4)_2 \cdot xH_2O$	25.46	(Musvoto et al., 2000)
Calcite	$Ca^{2+} + CO_3^{2-} \leftrightarrow CaCO_3$	8.42–8.22–8.48	(Musvoto et al., 2000, Stumm and Morgan, 1981)

system. Therefore, this value was chosen as the highest level considered, and two lower values were identified (each by a -0.8 step: 1.53 and 0.73) to end testing with molar ratio lower than 1. On the other hand, a NH_4/P molar ratio lower than the initial one does not make much practical sense, since such an amount of ammonium in solution would be too low to allow struvite precipitation. In this case, the observed ratio initial value was maintained as the lowest level, and two other higher levels were chosen (each with step of $+1$: 2.5, 3.5) to test the effect of ammonium to P ratio in solution. As far as pH, the lowest test level was chosen as 8.5, since this was the point at which precipitation started to be significant enough to be observed and generate filterable precipitate. The highest level was set as 9.5 because after this point it was observed that most of the precipitate consisted of carbonates. The second order responses for the chosen predictors are formulated according to Eq. (6):

$$Y = \beta_0 + \sum_{i=1}^3 \beta_i X_i + \sum_{i < j} \beta_{ij} X_i X_j + \sum_{i=1}^3 \beta_{ii} X_i^2 \quad (6)$$

The R programming language has been used to perform RSM and statistical analysis of process data (available online as The Comprehensive R Archive Network, CRAN, <https://cran.r-project.org/>). R is a powerful free software environment developed specifically for statistical modeling, computing and graphics. It supports the use of different packages with built-in functions designed for particular purposes. The “RSM” package (Lenth, 2012) was used in this work, as it contains valuable functions for BBD and RSM applications.

4. Results and discussion

4.1. Chemical equilibrium modeling

The results of PHREEQC modeling are summarized in Table 3. The model calculated ion speciation and struvite SI values for all runs. It

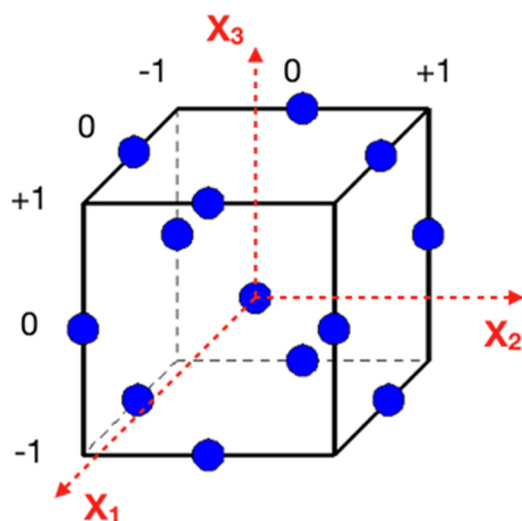


Fig. 1. Box-Behnken test design scheme for 3 factors.

can be seen that all calculated SI values are positive, which suggests that struvite precipitation could, in theory, occur in the system. However, some of these SI values are very low (e.g. Table 3, 9th run), meaning that in those cases there is just a slight possibility of struvite formation, will probable predominance of calcium phosphate and other P-compounds in the final precipitate. Furthermore, the range of SI values obtained during the entire set of tests is not notably high (<1 for all of them), in contrast with most literature results that generally report higher values (specifically, >1) for struvite SI. This may be due to the fact that most literature studies have worked with wastewater having considerably higher phosphorus concentrations than the one used herein (300–500 mg/l compared to around 40 mg/l in our case) due to the fact that these works usually dealt with anaerobic digester filtrate, much higher in P content. Fang et al. (2016) suggested that as the initial concentration of phosphorus increases, the value of SI will also increase. This can be true at least up to concentrations of around 1000 mg/l at which the SI will start to decrease.

The phosphorus removal percentage and amount of total phosphorus precipitated, both calculated based on the result of PHREEQC modeling, have been compared to measured values in tests, and the result is shown in Fig. 2. Although some inaccuracies and errors are unavoidable in a comparison between numerically calculated and experimentally measured values, it can be concluded that the PHREEQC software had an adequate performance on simulating the experiments. Notwithstanding sample triplicate repetition, some part of the errors can in fact be attributed to measurement errors in the lab (e.g. experiment 5 showing as an outlier in Fig. 2).

4.2. Analysis of final precipitates

Analysis of final precipitates using Fourier Transform Infrared (FTIR) spectroscopy shows a very similar pattern for all experiments. The results for experiment 8 (the one with the highest amount of precipitate obtained) are presented in Fig. 3. These confirm the presence of phosphate groups (PO_4^{3-}) and water molecules within, by showing these molecules' associated peaks at around 1000–1100 and 3500–3600 cm^{-1} respectively (Soptrajanov et al., 2004) (Fig. 3a, prior to TGA). The FTIR spectrum in the range 1200–2000 cm^{-1} has a more

Table 3

Values of predictor variables with their coded values in the Box-Behnken design and results of PHREEQC modeling for response variables.

Run	Ca/Mg	NH_4/P	pH	X_1	X_2	X_3	SI	P rem. %
1	0.73	1.5	9.0	-1	-1	0	0.48	82.46
2	2.33	1.5	9.0	1	-1	0	0.17	72.76
3	0.73	3.5	9.0	-1	1	0	0.84	82.15
4	2.33	3.5	9.0	1	1	0	0.54	72.20
5	0.73	2.5	8.5	-1	0	-1	0.54	70.28
6	2.33	2.5	8.5	1	0	-1	0.21	58.03
7	0.73	2.5	9.5	-1	0	1	0.60	92.08
8	2.33	2.5	9.5	1	0	1	0.32	86.33
9	1.53	1.5	8.5	0	-1	-1	0.13	62.40
10	1.53	3.5	8.5	0	1	-1	0.49	61.60
11	1.53	1.5	9.5	0	-1	1	0.22	88.59
12	1.53	3.5	9.5	0	1	1	0.58	88.29
13	1.53	2.5	9.0	0	0	0	0.52	75.86
14	1.53	2.5	9.0	0	0	0	0.52	75.89
15	1.53	2.5	9.0	0	0	0	0.52	75.89

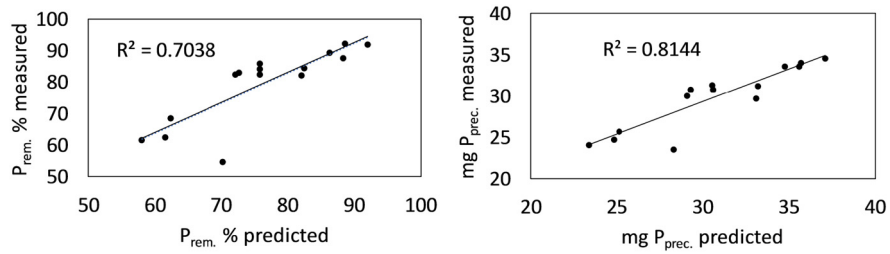


Fig. 2. Comparison of predicted results (PHREEQC) with measured values, left: P removal %, right: mg of P precipitated in the system.

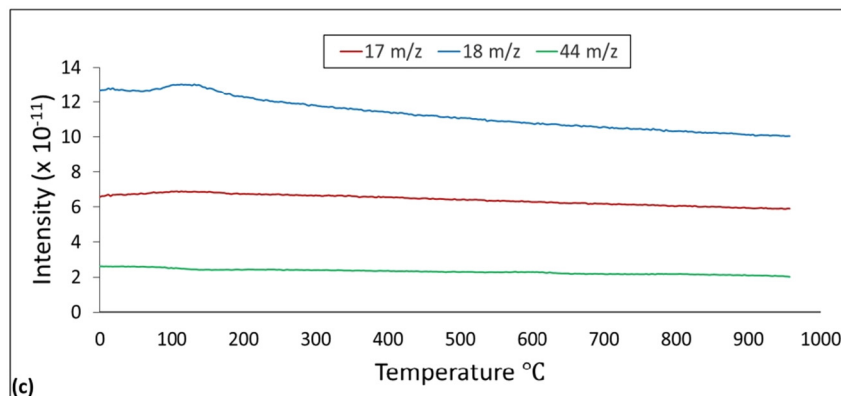
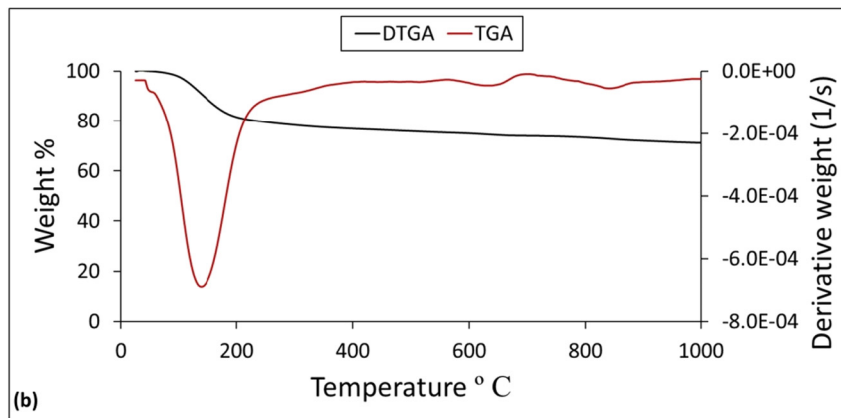
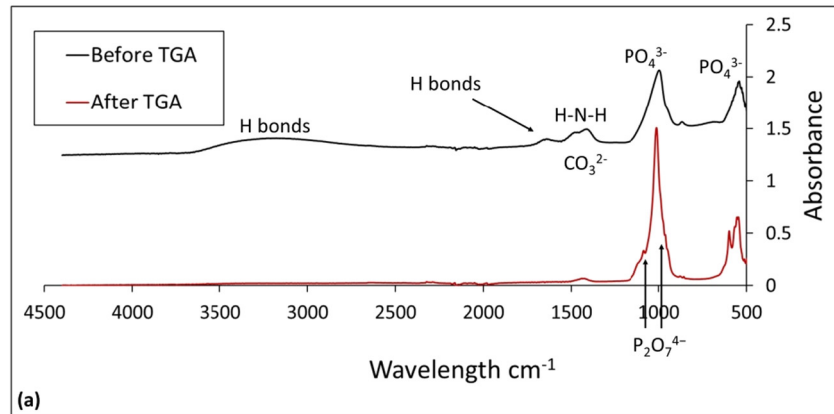


Fig. 3. FTIR spectra (a), TGA (b) and MS (c) of precipitates from aerobic sludge sample.

Table 4
ICP-AES and elemental analysis of the final precipitates.

Ions	mole/kg
Ca	4.48
Mg	0.59
P	3.82
N	0.33
C	3.02

Table 5
ANOVA analysis for the saturation index (SI).

	Estimate	Std. Err	t value	Pr(> t)	
Intercept	5.2e-01	1.2910e-03	402.7903	1.790e-12	***
X1	-1.525e-01	7.9057e-04	-192.8989	7.104e-11	***
X2	1.812e-01	7.9057e-04	229.2651	2.996e-11	***
X3	4.375e-02	7.9057e-04	55.3399	3.644e-08	***
X1.X2	2.500e-03	1.1180e-03	2.2361	0.07559	
X1.X3	1.250e-02	1.1180e-03	11.1803	9.989e-05	***
X2.X3	-2.095e-17	1.1180e-03	0.0000	1.00000	
X1^2	2.500e-02	1.1637e-03	21.4834	4.053e-06	***
X2^2	-3.750e-02	1.1637e-03	-32.2252	5.406e-07	***
X3^2	-1.275e-01	1.1637e-03	-109.5656	1.201e-09	***
Adjusted R-squared		0.9999			
F-statistic		1.184e+04			
p-value		2.809e-10			
Lack of fit Pr(> t)		2.2e-16			

complicated explanation. Visible peaks in this range appear at 1440 and 1550 cm^{-1} and could be associated to the presence of H-N-H bonds. Nonetheless, carbonate groups (CO_3^{2-}) also show similar peaks in this range (Berzina-Cimdina and Borodajenko, 2012). The small peak showing at 1650 cm^{-1} could be related to the H-bonds of the amorphous phases, therefore, peaks in this range seem to be the results of individual peaks convolution, related to each group. This could suggest the contemporary presence of struvite, ACP and calcite at the same time in the final precipitate. A TGA/DTGA (Derivative TGA) analysis of precipitates (Fig. 3b) highlighted a weight loss within their mass at around 150 °C, which could be related to the loss of both ammonia and water. Other two weight losses are identified at around 650 and 800 °C, and these are typical weight losses of carbon dioxide, related to the presence of calcite (Dubberke and Marks, 1992). Fig. 3c shows the MS analysis of the precipitate. The results of TGA can therefore be confirmed by MS, due to the presence of a peak in the graph with mass-to-charge ratio of 17 m/z ($\text{NH}_3 + \text{H}_2\text{O}$) and two very small peaks for the mass-to-charge ratio of 44 m/z (CO_2).

The ICP-AES and elemental analysis of the final precipitates (Table 4, also referred to the outcome of experiment 8) shows the presence of P, Mg and N that are related to the presence of struvite, although a high amount of Ca is also detected. The higher molar ratio of Ca corresponding to P could be due to calcite precipitation, in addition to ACP, justified by the higher P content in comparison to Mg and N.

Very similar results have been obtained for practically all tests, with the main difference laying in the intensity of the peaks in FTIR results. As pH increases from 8.5 to 9.5, the peaks corresponding to carbonate and phosphate groups intensify. This suggests a higher phosphorus content in final precipitates, leading to higher P removal percentage. However, it should be kept in mind that intensified peaks of carbonate also indicate high calcite precipitation.

4.3. Statistical modeling and analysis

4.3.1. RSM analysis

Results of the RSM analysis were obtained for each one of the response variables in this study. Analysis of variance (ANOVA) of the RSM models shows significant tests for all parameters, the main effects of predictors, two-way interactions and quadratic terms. Results for SI show (Table 5) that all terms, except for two of the interactions (Ca/Mg, NH_4/P and $\text{NH}_4/\text{P}, \text{pH}$), are significant, and should be taken into account in the model. The adjusted R-squared value is quite good (0.99), but the ANOVA analysis shows a lack of fit, which may be attributed to the center points of the scheme. All three center points have the same value for the SI since they are calculated under the same conditions by PHREEQC. The plot of the residuals vs fitted values (Fig. 4a) confirms the good fit of the model, as there is no specific pattern in the plot. The same analysis for the second response (phosphorus removal percentage) indicates that the only parameters significantly affecting it are pH and its quadratic term (Table 6). This was an unexpected result, especially in comparison to other literature studies. The authors believe two reasons might be involved. One, as mentioned before, concerns the concentrations of constituent ions, relatively low compared to similar studies, which could lead to magnification of the pH effect, compared to others. On the other hand, the values of the second response are obtained experimentally, unlike those of the first response, which were predicted by PHREEQC. Measurement errors and lower accuracy due to experimental conditions for second response values, compared to the first ones, could lead to such observed differences between fitted models. Nevertheless, the insignificant lack of fit suggested by ANOVA, and the residual-vs-fitted plot for the second response confirm the goodness of the final model (Fig. 4b).

The fitted response for SI and P removal percentage is presented with the following RSM equations:

$$SI = 0.52 - 0.1525X_1 + 0.1812X_2 + 0.04375X_3 + 0.0125X_1X_3 + 0.025X_1^2 - 0.0375X_2^2 - 0.1275X_3^2 \quad (7)$$

$$P_{rem} = 84.06 + 14.25X_3 - 7.475X_3^2 \quad (8)$$

RSM shows that for both responses, the stationary point of the fitted response surface is a saddle point, i.e. is a type of stationary point that is neither a maximum nor a minimum. Therefore, depending on the direction towards which one moves from that point, the response variable can either increase or decrease (Fig. 5). Stationary points for saturation index and phosphorus removal percentage response variables are Ca/

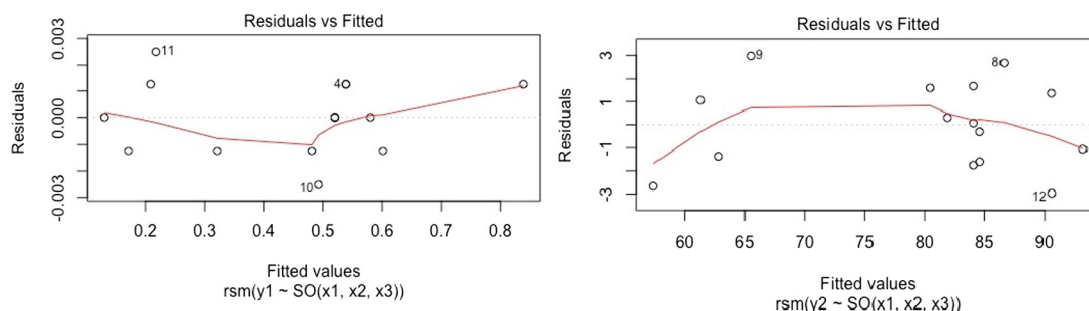


Fig. 4. Residuals versus fitted values for response variables, a) SI, b) P removal %.

Table 6
ANOVA analysis for P removal percentage.

	Estimate	Std. Err	t value	Pr(> t)	
Intercept	84.0600	1.8078	46.4986	8.689e-08	***
X1	0.3675	1.1070	0.3320	0.753379	
X2	-1.7050	1.1070	-1.5401	0.184154	
X3	14.2500	1.1070	12.8721	5.039e-05	***
X1.X2	0.3600	1.5656	0.2299	0.827246	
X1.X3	-2.3400	1.5656	-1.4946	0.195243	
X2.X3	0.3950	1.5656	0.2523	0.810852	
X1^2	-2.2450	1.6295	-1.3777	0.226765	
X2^2	1.0650	1.6295	0.6536	0.542251	
X3^2	-7.4750	1.6295	-4.5872	0.005908	**
Adjusted R-squared		0.9296			
F-statistic		21.53			
p-value		0.001754			
Lack of fit Pr(> t)		0.1746929			

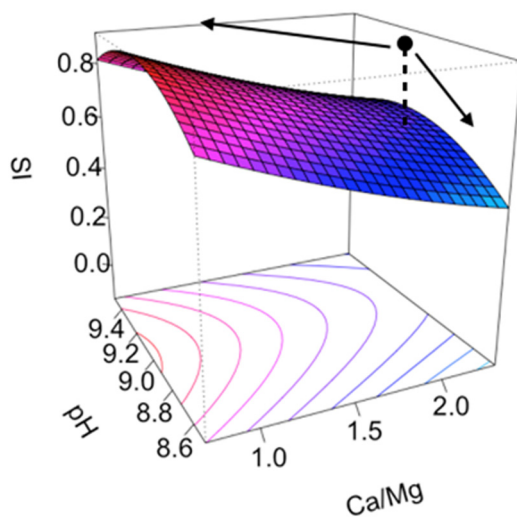


Fig. 5. Saddle point obtained for the response variables.

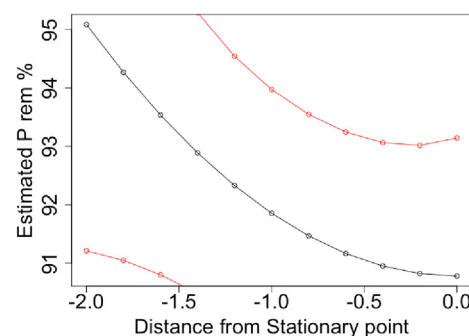
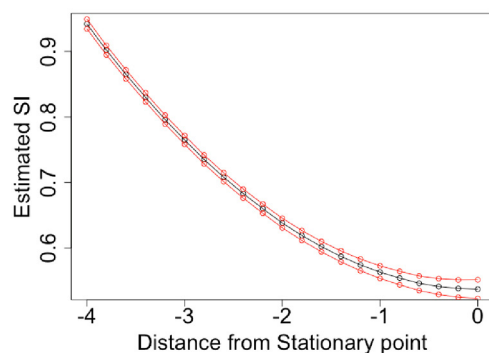
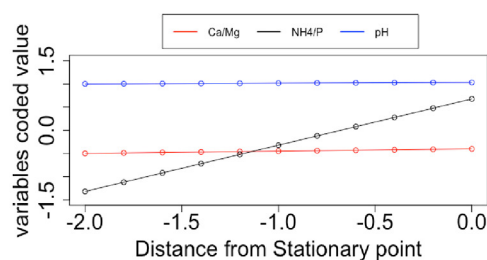
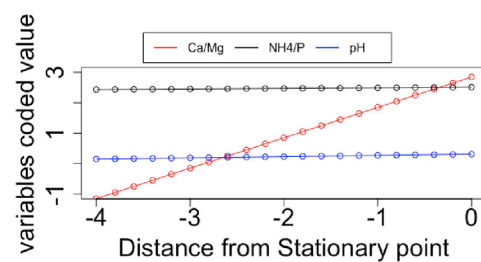


Fig. 6. Top: Predictor variables coded values versus their distance from the stationary point, left: SI, right: P removal %. Bottom: Estimated response variables vs distance from the stationary point, left: SI, right: P removal %.

Mg: 3.8, NH_4/P : 5, pH: 9.15 and Ca/Mg:1.2, NH_4/P :3.17, pH: 9.5 respectively. It should be understood that for some of the predictors, the corresponding stationary point may lay outside the region of experiments design. Based on these stationary points, the ridge analysis method was then used to search for the optimum values of the response variables within the experimental design region, as described hereafter.

4.3.2. Ridge analysis

Ridge analysis is a powerful method for exploring optimum values of a fitted response surface, which has a stationary point outside of the experimental design region. Results of the ridge analysis for both SI and P removal efficiency indicate the directions towards which optimum values of the response variables may be sought and found. Fig. 6 (top) plots coded values of predictors vs. distance from the stationary point. It can be seen that the further one moves from the stationary point, the only predictor variables affecting response variables are Ca/Mg and NH_4/P for SI and P removal efficiency, respectively. On the other hand, this suggests that to optimize the SI value one needs to move away from the stationary point towards the direction in which Ca/Mg is decreasing. A similar pattern is true for the P removal efficiency, except for the search direction that in this case is towards decreasing NH_4/P values. Fig. 6 (bottom) illustrates plots of estimated values of response variables at increasing distance from the stationary point. Red lines represent standard error values, very limited in the case of SI, contrary to that for P removal, for which error first decreases, and increases afterwards as the distance from stationary point keeps increasing. This, therefore, limits the maximum distance one may choose to consider moving away from the stationary point. To avoid high error values for estimated response variables, such distance needs to be kept in a specific range (between 1 and 1.5, in coded value units, to the center of the BBD design).

Figs. 7 and 8 illustrate the perspective response surfaces for SI and P removal efficiency, respectively. Locations of the stationary points and the directions towards which optimum values will be obtained are also indicated. Each surface represents the plot of a response variable, based on two of the predictor variables intersected, where the remaining third variable is at its stationary point. Fig. 7, as an example, shows

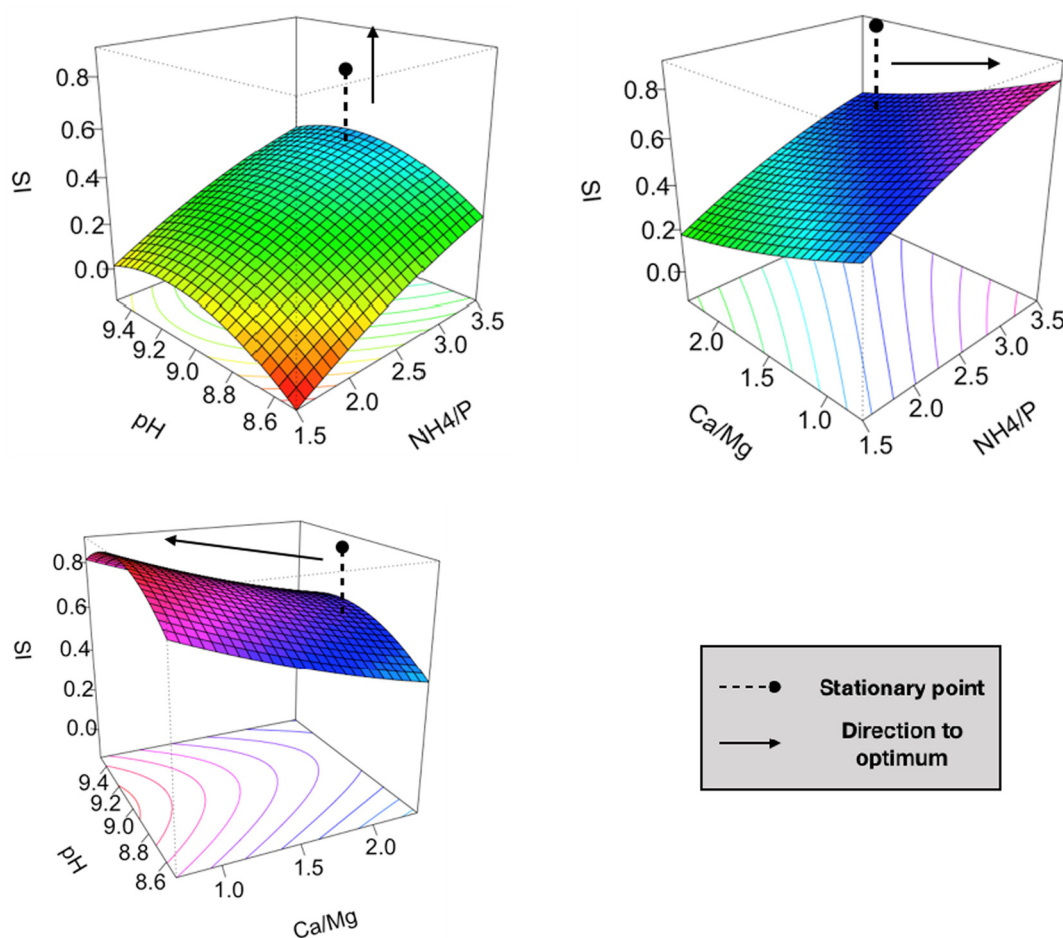


Fig. 7. Response surface perspectives for SI based on predictor variables.

that P removal efficiency as response variable is highly affected by pH, and not much by the other two predictors.

Table 7 shows the optimum values (ranges) of the predictor variables obtained by RSM and ridge analysis. It can be concluded that by increasing the pH value to 9 both responses are increasing. However, their response changes past that value: above pH = 9; P removal efficiency will still increase, but the value of struvite SI will decrease. This means that after this point, the possibility of struvite precipitation will decrease, and calcium phosphate compounds will be mostly responsible for the increase of P removal percentage. The optimum Ca/Mg ratio for SI is 0.8, aligned with other literature findings, usually suggesting a value of <1 (Crutchik and Garrido, 2011).

Obviously, higher P removal efficiency will need at this point higher Ca/Mg ratios, as such conditions will promote calcium phosphate precipitation. Optimum values for the NH_4/P ratio were determined as 2 and >3.5 for P removal efficiency and SI, respectively. Although the optimal value of NH_4/P for SI is off the design region of the experiments performed, results suggest that to achieve higher struvite precipitation possibility, ammonium content of the solution needs to be sufficiently higher than phosphorus content. This can be explained by the fact that phosphorus also gets involved in other competitive reactions, mostly for calcium phosphate compounds formation. The RSM model, however, suggests that a lower value of NH_4/P ratio should be targeted to increase P removal efficiency, as lower values favor precipitation of calcium compounds other than struvite (Capdevielle et al., 2013). The optimum SI calculated for Ca/Mg = 0.8, NH_4/P = 3.5 and pH = 9 is 0.82, with an associated P removal efficiency of 84.06%. On the other hand, Ca/Mg = 1.2, NH_4/P = 2 and pH = 9.5 will increase P removal efficiency to 90.83%, but at the same time will lead to a lower SI of 0.39.

In conclusion, keeping the Ca/Mg ratio lower than 1, NH_4/P higher than 3 and pH at 9 will achieve better struvite precipitation, although that will occur at the cost of a lower total phosphorus removal. The model therefore indicates that in the examined conditions, an ideal struvite precipitation process is not sufficient alone, to maximize P removal for the purpose of meeting or exceeding its removal limits, as obtaining a purer struvite product would necessarily lead to lower overall P removal efficiencies.

5. Conclusions

In this study, chemical modeling and Response Surface Methodology were combined to investigate the optimum conditions under which high phosphorus recovery in the form of struvite (or other compounds) can be achieved in the wastewater treatment facility under study. A Box-Behnken Design testing was applied with pH, Ca/Mg and NH_4/P as the 3 predictor variables. Values of the struvite saturation index calculated by chemical equilibrium modeling (PHREECC) and phosphorus removal percentage were chosen as system response variables. Ridge analysis was used in order to investigate the ultimate optimum values for the predictor variables when the stationary point is a saddle point. The results showed the direction towards which one needs to move from the obtained stationary point in order to further improve the optimum values. BBD results show optimum values of pH = 9, Ca/Mg = 0.8, NH_4/P > 3.5 and pH = 9.5, Ca/Mg = 1.2, NH_4/P = 2 for SI and P removal efficiency, respectively. It can be therefore concluded that in order to achieve higher phosphorus recovery in the form of pure struvite, the Ca/Mg ratio needs to be kept lower than 1 and the pH at closely around 9. For pH levels greater than this value, very high phosphorus removal

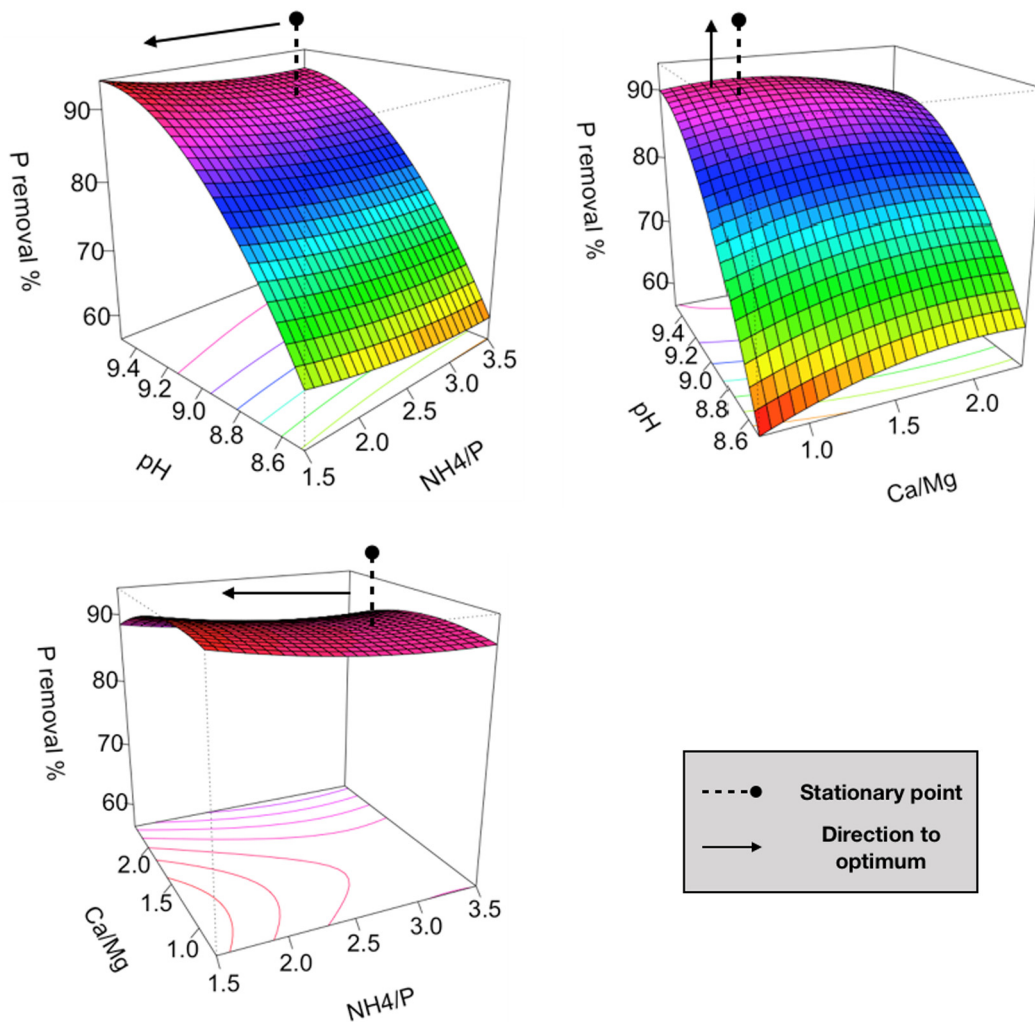


Fig. 8. Response surface perspectives for P removal percentage based on predictor variables.

(>90%) can still be achieved, but with a low probability of obtaining pure struvite precipitation.

Combined results of RSM and chemical modeling of P compounds precipitation could be very helpful for the design and optimization of phosphorous removal and recovery processes, especially when the latter is actively pursued. Optimized values/ranges of significant process variables will lead to a more efficient and productive process design for recovering phosphorus in the form of struvite or other compounds as valuable products.

Funding

This study was supported by a research grant from the CARIPLo Foundation (grant 2014/0528) to the University of Pavia, Department of Civil Engineering & Architecture (P.I. Prof. Andrea G. Capodaglio). The work of Céline Vaneckhaute and Peter Vanrolleghem is supported

by a NSERC (Canada) project grant. Dr. Vanrolleghem holds, and is supported by, the Canada Research Chairs on water quality modeling.

Acknowledgments

Mr. Daneshgar received full PhD scholarship support from the abovementioned CARIPLo Foundation grant. The authors thank the WWTP operator in Italy for granting access and for the possibility of conducting extensive testing on the facility. Université Laval in Quebec City (Canada) hosted Mr. Daneshgar for a sabbatical period during his PhD work.

References

- Bendoricchio, G., Di Luzio, M., Baschieri, P., Capodaglio, A.G., 1993. Diffuse pollution in the lagoon of Venice. *Water Sci. Technol.* 28 (3–5), 69–78 Retrieved from. <http://www.iwaponline.com/wst/02803/wst028030069.htm>.
- Berzina-Cimdina, L., Borodajenko, N., 2012. Research of calcium phosphates using fourier transform infrared spectroscopy. *Infrared Spectroscopy - Materials Science, Engineering and Technology*. <https://doi.org/10.5772/36942>.
- Bhuiyan, M.I.H., Mavnic, D.S., Beckie, R.D., 2007. A solubility and thermodynamic study of struvite. *Environ. Technol.* 28, 1015–1026.
- Bhuiyan, M.I.H., Mavnic, D.S., Beckie, R.D., 2008. Nucleation and growth kinetics of struvite in a fluidized bed reactor. *J. Cryst. Growth* 310 (6), 1187–1194. <https://doi.org/10.1016/j.jcrysgro.2007.12.054>.
- Borgerding, J., 1972. Phosphate deposits in digestion systems. *J. Water Pollut. Control Fed.* 44 (5), 813–819. [https://doi.org/10.1016/S0043-1354\(01\)00143-9](https://doi.org/10.1016/S0043-1354(01)00143-9).
- Box, G.E.P., Behnken, D., 1960. Some new three level designs for study of quantitative variables. *Technometrics* 2, 455–475.

Table 7
Optimum values for predictor variables.

Predictor variable	Optimum value for saturation index (SI)	Optimum value for P removal %
Ca/Mg	0.8	1.2
NH ₄ /P	>3.5	2
pH	9	9.5

- Box, G.E.P., Wilson, K.B., 1951. On the Experimental Attainment of Optimum Conditions. Of the Royal Statistical Society, Series B Vol. XIII (1), 1–38 <https://doi.org/10.1111/j.2517-6161.1951.tb00067.x>.
- Capdevielle, A., Sýkorová, E., Biscans, B., Béline, F., Daumer, M.L., 2013. Optimization of struvite precipitation in synthetic biologically treated swine wastewater-determination of the optimal process parameters. *J. Hazard. Mater.* 244–245, 357–369. <https://doi.org/10.1016/j.jhazmat.2012.11.054>.
- Capodaglio, A.G., Muraca, A., Becchi, G., 2003. Accounting for water quality effects of future urbanization: diffuse pollution loads estimates and control in Mantua's lakes (Italy). *Water Sci. Technol.* 47, 291–298.
- Cordell, D., Drangert, J.O., White, S., 2009. The story of phosphorus: global food security and food for thought. *Glob. Environ. Chang.* 19 (2), 292–305. <https://doi.org/10.1016/j.gloenvcha.2008.10.009>.
- Crutchik, D., Garrido, J.M., 2011. Struvite crystallization versus amorphous magnesium and calcium phosphate precipitation during the treatment of a saline industrial wastewater. *Water Sci. Technol.* 64 (12), 2460–2467. <https://doi.org/10.2166/wst.2011.836>.
- Daneshgar, S., Callegari, A., Capodaglio, A., Vaccari, D., 2018a. The potential phosphorus crisis: resource conservation and possible escape technologies: a review. *Resources* 7, 37. <https://doi.org/10.3390/resources7020037>.
- Daneshgar, S., Buttafava, A., Callegari, A., Capodaglio, A.G., 2018b. Simulations and laboratory tests for assessing phosphorus recovery efficiency from sewage sludge. *Resources* 7, 54.
- Daneshgar, S., Buttafava, A., Capsoni, D., Callegari, A., Capodaglio, A.G., 2018c. Impact of pH and ionic molar ratios on phosphorus forms precipitation and recovery from different wastewater sludges. *Resources* 7, 71. <https://doi.org/10.3390/resources7040071>.
- Desmidt, E., Ghyselbrecht, K., Zhang, Y., Pinoy, L., Van Der Bruggen, B., Verstraete, W., Rabaey, K., Meesschaert, B., 2015. Global phosphorus scarcity and full-scale P-recovery techniques: a review. *Crit. Rev. Environ. Sci. Technol.* 45 (4), 336–384. <https://doi.org/10.1080/10643389.2013.866531>.
- Doyle, J.D., Parsons, S.A., 2002. Struvite formation, control and recovery. *Water Res.* 36 (16), 3925–3940. [https://doi.org/10.1016/S0043-1354\(02\)00126-4](https://doi.org/10.1016/S0043-1354(02)00126-4).
- Dubberke, W., Marks, V.J., 1992. Thermogravimetric analysis of carbonate aggregate. *Transp. Res. Rec.* (1362), 38–43 Retrieved from: <http://trid.trb.org/view.aspx?id=370975>.
- Fang, C., Zhang, T., Jiang, R., & Ohtake, H. (2016). Phosphate enhance recovery from wastewater by mechanism analysis and optimization of struvite settleability in fluidized bed reactor. *Sci. Rep.*, 6(August), 1–10. doi:<https://doi.org/10.1038/srep32215>.
- Galbraith, S.C., Schneider, P.A., 2014. Modelling and simulation of inorganic precipitation with nucleation, crystal growth and aggregation: a new approach to an old method. *Chem. Eng. J.* 240, 124–132. <https://doi.org/10.1016/j.cej.2013.11.070>.
- Galbraith, S.C., Schneider, P.A., Flood, A.E., 2014. Model-driven experimental evaluation of struvite nucleation, growth and aggregation kinetics. *Water Res.* 56, 122–132. <https://doi.org/10.1016/j.watres.2014.03.002>.
- Hao, X.D., Wang, C.C., Lan, L., Van Loosdrecht, M.C.M., 2008. Struvite formation, analytical methods and effects of pH and Ca²⁺. *Water Sci. Technol.* 58 (8), 1687–1692. <https://doi.org/10.2166/wst.2008.557>.
- Harada, H., Shimizu, Y., Miyagoshi, Y., Matsui, S., Matsuda, T., Nagasaka, T., 2006. Predicting struvite formation for phosphorus recovery from human urine using an equilibrium model. *Water Sci. Technol.* 54 (8), 247–255. <https://doi.org/10.2166/wst.2006.720>.
- Johnsson, M.S.-A., Nancollas, G.H., 1992. The role of brushite and octacalcium phosphate in apatite formation. *Crit. Rev. Oral Biol. Med.* 3 (1), 61–82. <https://doi.org/10.1177/10454411920030010601>.
- Le Corre, K.S., 2006. Understanding Struvite Crystallization and Recovery. PhD Thesis, School of Applied Science, Department of Sustainable Systems, Centre for Water Science. Cranfield University, Cranfield, UK.
- Le Corre, K.S., Valsami-Jones, E., Hobbs, P., Parsons, S.A., 2007. Kinetics of struvite precipitation: effect of the magnesium dose on induction times and precipitation rates. *Environ. Technol.* 28 (12), 1317–1324. <https://doi.org/10.1080/09593332808618891>.
- Lee, S.H., Yoo, B.H., Lim, S.J., Kim, T.H., Kim, S.K., Kim, J.Y., 2013. Development and validation of an equilibrium model for struvite formation with calcium co-precipitation. *J. Cryst. Growth* 372, 129–137. <https://doi.org/10.1016/j.jcrysgro.2013.03.010>.
- Lenth, R.V., 2012. Response-surface methods in R, using RSM. *J. Stat. Softw.* 32 (7), 1–17. <https://doi.org/10.18637/jss.v032.i07>.
- de Luna, M.D.G., Abarca, R.R.M., Su, C.C., Huang, Y.H., Lu, M.C., 2015. Multivariate optimization of phosphate removal and recovery from aqueous solution by struvite crystallization in a fluidized-bed reactor. *Desalin. Water Treat.* 55 (2), 496–505. <https://doi.org/10.1080/19443994.2014.915584>.
- Morse, G.K., Brett, S.W., Guy, J. a, Lester, J.N., 1998. Phosphorus removal and recovery technologies. *Sci. Total Environ.* 212, 69–81. [https://doi.org/10.1016/S0048-9697\(97\)00332-X](https://doi.org/10.1016/S0048-9697(97)00332-X).
- Munir, M.T., Li, B., Boiarkina, I., Baroutian, S., Yu, W., Young, R., 2017. Phosphate recovery from hydrothermally treated sewage sludge struvite precipitation. *Bioresour. Technol.* 239, 171–179. <https://doi.org/10.1016/j.biortech.2017.04.129>.
- Musvoto, E.V., Wentzel, M.C.M., Ekama, G. a M., 2000. Integrated chemical-physical processes modelling-II. Simulating aeration treatment of anaerobic digester supernatants. *Water Res.* 34 (6), 1868–1880.
- Parkhurst, D. L., & Appelo, C. A. J. (2013). Description of input and examples for PHREEQC Version 3 – A computer program for speciation, batch-reaction, one-dimensional transport, and inverse geochemical calculations. U.S. Geological Survey Techniques and Methods, book 6, chapter A43, 497 p. U.S. Geological Survey Techniques and Methods, Book 6, Chapter A43, 6–43A. doi:[https://doi.org/10.1016/0029-6554\(94\)90020-5](https://doi.org/10.1016/0029-6554(94)90020-5)
- Peng, L., Dai, H., Wu, Y., Peng, Y., Lu, X., 2018. A comprehensive review of phosphorus recovery from wastewater by crystallization processes. *Chemosphere* 197, 768–781. <https://doi.org/10.1016/j.chemosphere.2018.01.098>.
- Shalaby, M.S., 2015. Modeling and optimization of phosphate recovery from industrial wastewater and precipitation of solid fertilizer using experimental design methodology. *Chem. Biochem. Eng. Q. J.* 29 (1), 35–46. <https://doi.org/10.15255/CABEQ.2014.2107>.
- Soptrajanov, B., Stefov, V., Lutz, H.D., Engelen, B., 2004. Infrared and raman spectra of magnesium ammonium phosphate hexahydrate (struvite) and its isomorphous analogues. *Spectroscopy of Emerging Materials*, (1), pp. 299–308 <https://doi.org/10.1016/j.jmolstruc.2005.05.040>.
- Stumm, W., Morgan, J.J., 1981. *Aquatic Chemistry: An Introduction Emphasizing Chemical Equilibria in Natural Waters*. Wiley-Interscience, New York, USA.
- Taylor, A.W., Frazier, A.W., Gurney, E.L., 1963. Solubility products of magnesium ammonium and magnesium potassium phosphates. *Trans. Faraday Soc.* 59, 1580. <https://doi.org/10.1039/TF9635901580>.
- Türker, M., Çelen, I., 2007. Removal of ammonia as struvite from anaerobic digester effluents and recycling of magnesium and phosphate. *Bioresour. Technol.* 98 (8), 1529–1534. <https://doi.org/10.1016/j.biortech.2006.06.026>.
- US EPA (1978) United States Environmental Protection Agency, Method 365.3: Phosphorus, all forms (colorimetric, ascorbic acid, two reagent), accessible at https://www.epa.gov/sites/production/files/2015-08/.../method_365-3_1978.pdf (accessed on February 15th, 2016).
- US EPA (1991) MINTEQA2/PRODEFA2, A Geochemical Assessment Model for Environmental Systems: Version 3.0 User's Manual. EPA/600/3-91/021. ERL, Athens, GA.
- US Geological Survey (2013), PHREEQC (Version 3) – A computer program for speciation, batch-reaction, one-dimensional transport, and inverse geochemical calculations, (https://wwwbrr.cr.usgs.gov/projects/GWC_coupled/phreeqc/) (accessed on October 30th, 2017).
- Vaneekhaute, C., Claeys, F.H.A., Tack, F.M.G., Meers, E., Belia, E., Vanrolleghem, P.A., 2018. Development, implementation, and validation of a generic nutrient recovery model (NRM) library. *Environ. Model. Softw.* 99, 170–209. <https://doi.org/10.1016/j.envsoft.2017.09.002>.
- Wang, J., Burken, J. G., Zhang, X. (Jackie), Surampalli, R. (2005). Engineered struvite precipitation: impacts of component-ion molar ratios and pH. *J. Environ. Eng.*, 131(10), 1433–1440. doi:10.1061/(ASCE)0733-9372(2005)131:10(1433).
- Ye, X., Ye, Z.L., Lou, Y., Pan, S., Wang, X., Wang, M.K., Chen, S., 2016. A comprehensive understanding of saturation index and upflow velocity in a pilot-scale fluidized bed reactor for struvite recovery from swine wastewater. *Powder Technol.* 295, 16–26. <https://doi.org/10.1016/j.powtec.2016.03.022>.